14

Molecular modeling and OCT monitoring of optical clearing of human skin

© K.V. Berezin,[1] E.V. Grabarchuk,[2] A.M. Lichter,[2] K.N. Dvoretski,[3] Yu.I. Surkov,[1,4] V.V. Tuchin[1,4]

[1] Department of Physics, Saratov State University,
410012 Saratov, Russia
[2] Astrakhan Tatishchev State University,
414056 Astrakhan, Russia
[3] Saratov State Medical University named after V. I. Razumovsky
410012 Saratov, Russia
[4] Science Medical Center, Saratov State University,
410012 Saratov, Russia
e-mail: dcn@yandex.ru

Received December 31, 2023
Revised December 31, 2023
Accepted December 31, 2023

Using an optical coherence tomograph, the results of immersion optical clearing of human skin *in vivo* using an aqueous solution of glucosamine hydrochloride as a clearing agent were obtained. To assess the effectiveness of optical clearing, we determined the rate of decrease in the light scattering coefficient obtained using an averaged A-scan — a tomograph image in the dermis at a depth of 350 to 700 μm. Complex molecular modeling was carried out, which includes methods of classical molecular dynamics and methods of quantum chemistry HF/STO3G/DFT/B3LYP/6−311G(d) of intermolecular interaction of a number of clearing agents related to amino and imino sugars (glucosamine, galactosamine, 1-deoxynojirimycin) with fragment of collagen peptide $(GPH)_3$. Correlations have been established between the efficiency of optical clearing and such theoretical parameters as the average number of hydrogen bonds formed between clearing agents and a fragment of collagen peptide $(GPH)_3$ and the energy of intermolecular interaction of clearing agents with the same peptide. Using the constructed correlation, the optical clearing efficiency values for the molecules of glucosamine, galactosamine and 1-deoxynojirimycin were predicted.

Keywords: molecular modeling, optical clearing of human skin, hydrogen bonds, molecular dynamics, quantum chemistry, amino sugars.

DOI: 10.21883/0000000000

Introduction

Application of modern methods of photomedicine and biomedical optics for the diagnosis and treatment of diseases is fraught with difficulties arising from the strong light scattering in the UV, visible and near-IR ranges, characteristic of the skin and many other soft and hard tissues [1]. Such scattering occurs due to the heterogeneity of refraction indices at the boundaries of various macromolecular structures, mainly on collagen fibers, which are primarily responsible for light scattering in the skin [2]. These difficulties, in particular, can be overcome by local delivery of biocompatible molecular agents into the tissue, which to some extent contributes to its optical clearing [1,3–6]. A lot of general scientific works — analytical reviews and monographs [1,3–11] have been devoted to the experimental study of optical clearing of various tissues *in vivo*, *ex vivo* and *in vitro*, which proves the relevance of the problem. Many articles present interesting applications of the optical clearing method or prove its versatility and multimodality. For example, forensic studies have described the use of optical coherence tomography (OCT) for postmortem clear visualization of the perinatal dura mater and superior sagittal sinus in newborns [12], and the work [13] a fast and universal method of optical clearing was presented. The work [14] evaluates the synergistic effect of a clearing agent (PEG-400), two penetration enhancers (triazine and 1,2-propanediol) and physical massage on the effectiveness of optical clearing of rat skin using OCT. The work [15] presents a mathematical model for solving the inverse problem of the interaction of light with biological tissue to determine the kinetics of scattering and absorption coefficients during optical clearing, taking into account the osmotic pressure of the optical clearing agent. Two OCT-based approaches for non-invasive identification of local molecular diffusion of clearing agents are described in [16]. Studies of diabetes mellitus on laboratory mice have shown a significant difficulty in the diffusion of clearing agents into glycated tissues [17]. The mechanisms of optical skin clearing with glycerol and the radiographic agent Omnipaque ™ as clearing agents were studied using two-photon excitation autofluorescence and second harmonic generation methods [18]. Using multiphoton tomography, the authors [19] examined the mechanisms of optical clearing in collagen tissue in normal and glycated states. The dehydrating properties of clearing agents have been studied in [20]; it was noted that dehydration is only one of the potential mechanisms of optical clearing of biological

tissues. Another mechanism is an increase in the refraction index of tissue fluid due to the diffusion of the clearing agent into the skin. This leads to improved optical matching between the skin tissue matrix (components of epidermal cells, basement membrane, fibrillar collagens and associated dermal proteins) and the surrounding tissue fluid. Another mechanism that can influence the process of optical clearing is the reversible dissociation of collagen fibrils [21], which is carried out due to the dehydration of collagen itself [22], and potentially the subsequent partial replacement of bound water with molecules clearing agent. In the work [23], using confocal RS microscopy *ex vivo*, we studied the movement of water in the skin of a pig's ear under the influence of 70% aqueous solution of glycerol and Omnipaque^{TM} 300. It is noted that weakly bound and strongly bound types of water together account for approximately 93% of the total water content in the skin, and they are mainly involved in interaction with clearing agents.

Further research in this area is aimed at understanding the physical and biophysical processes underlying the mechanisms of optical clearing at the molecular level [4,6,24–27], which, in turn, should allow to find new effective clearing agents that have specified properties and are optimal for a specific type of fabric.

This work describes the molecular mechanisms of optical clearing of human skin *in vivo* using the effect of an aqueous solution of glucosamine hydrochloride as an example. Glucosamine is an amino sugar and is one of the most common monosaccharides [28], which is important in the synthesis of glycosylated proteins and lipids. In medicine, glucosamine hydrochloride is used as a health supplement [29]. As an optical clearing agent, it is of interest, since it belongs to another group of previously studied sugars (mono, disaccharides), which have shown a high degree of efficiency in optical clearing of human skin.

For the first time, molecular models of complex compounds of glucosamine, galactosamine and 1-deoxynodirimycin molecules with a collagen peptide fragment were constructed. The parameters of intermolecular interaction were calculated, and based on the correlation data, the efficiency of optical clearing for the molecules of glucosamine, galactosamine and 1-deoxynodirimycin was theoretically predicted.

1. Materials and methods

An aqueous solution of glucosamine hydrochloride (60%) was used to study the optical clearing of human skin of healthy volunteers.

The glucosamine hydrochloride solution was prepared by precise weighing: on a microanalytical balance (DA-225DC with calibration (0.001 g), Bel Engineering, Italy). The components of the solution were weighed, which were then transferred to a volumetric flask for dissolution and mixed thoroughly using a vortex mixer.

The refraction index was measured using an Atago DR-M2 1550 multi-wave Abbe refractometer (Atago, Japan) at a wavelength of 930 nm at a temperature of 23.8°. The refraction index values of an aqueous solution of glucosamine hydrochloride are given in Table 1. For comparison, the table shows the characteristics of two more clearing agents studied in [25], the osmolality of which differs significantly from glucosamine hydrochloride.

OCT was used to evaluate the optical clearing properties of glucosamine hydrochloride when applied topically to the skin *in vivo*. The OCP930SR optical coherence tomograph (Thorlabs, USA) had the following parameters: central radiation wavelength 930 $\pm$ 5 nm, axial and lateral resolution 6.2 and 9.6 μm respectively (in air), scanning area length 2 mm.

The study was conducted in accordance with the Declaration of Helsinki and approved by the Ethics Committee of the Saratov State Medical University named after V.I. Razumovsky (№ 11 dated August 7, 2022). Measurements were taken on the skin of the back of the forearm. The stratum corneum in this area of the skin was previously removed with medical tape. Two-dimensional scans (B-scans) of the area under study were recorded before exposure to optical clearing agents, then during 60 min exposure with an interval of 3 min. Four volunteers aged from 35 to 55 years, of both sexes, took part in the measurements. A total of five measurements were carried out for this immersion agent.

According to the single scattering model, the recorded OCT signal [16,31–34]:

$$R(z) \sim \exp(-\mu_t z), \tag{1}$$

where the attenuation coefficient

$$\mu_t = \mu_s + \mu_s, \tag{2}$$

z — is scanning depth.

Since the skin absorption coefficient μ_a is significantly less than the scattering coefficient μ_s [1], the attenuation coefficient μ_t can be considered approximately equal to the scattering coefficient, so $R(z)$ can be approximated by the expression [35]

$$R(z) = A\exp(-\mu_s z) + B, \tag{3}$$

where A — coefficient of proportionality equal to $P_0 a(z)$, P_0 — optical power of the beam incident on the surface of the tissue, $a(z)$ is determined by the local ability of the tissue to scatter light back, which depends on the local change in the refraction index, and B — background signal. The selection of coefficients in the given expression to approximate the experimental curve allows us to estimate the depth-averaged scattering coefficient of the tissue sample.

2. Experimental results

Figure 1 shows the analyzed section of the OCT image (B-scans), as well as the averaged A-scan OCT signal

Table 1. Physical properties of clearing agents

Immersion Agent	Chemical formula	Molecular weight ($g \cdot mol^{-1}$)of	Refractive index	Osmolality (mOsm/kg water)
Glucosamine hydrochloride aqueous solution (60%)	$C_6H_{13}NO_5^*$	179.17*	1.4304	2782**
Sucrose aqueous solution (60%)	$C_{12}H_{22}O_{11}^*$	342.30*	1.4310 [25]	1753***
Omnipaque^{TM} 300	$C_{19}H_{26}I_3N_3O_9^*$	821.14*	1.4275 [25]	672 [30]

Note. * — designations and meanings are given for the ground substances in solution; ** — calculated value in the small dissociation approximation; *** — calculated value.

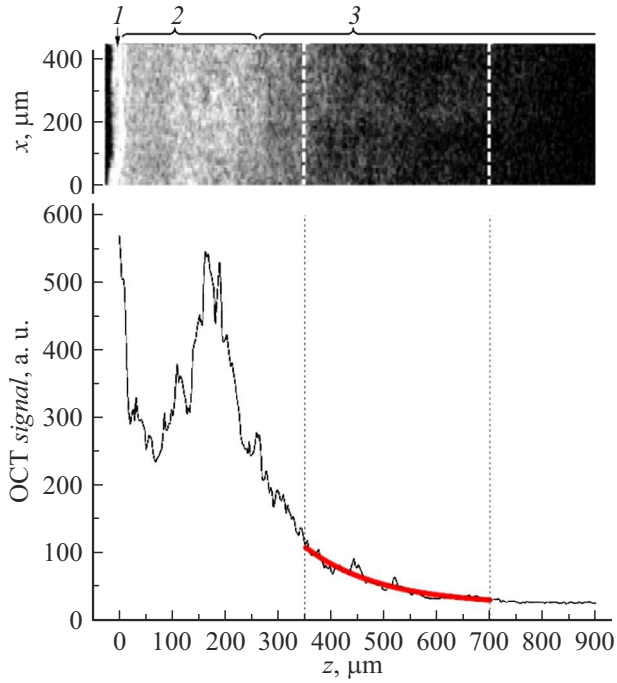

Figure 1. Measurements of the scattering coefficient of μ_s on the dermis after application of a glucosamine hydrochloride solution to the surface based on analysis of the OCT signal distribution averaged over depth using a single scattering model. Above are fragments of a skin B-scan *in vivo*, from which the OCT signal was averaged. The numbers indicate the layers of the skin: stratum corneum (*1*), epidermis (*2*) and dermis (*3*). Bottom — distribution of the averaged OCT signal over depth (thin curve) and the result of approximation according to the single scattering model (thick curve). The dashed lines in the figures indicate the boundaries of the sections (from 350 to 700 μm) on which the value of μ_s was estimated.

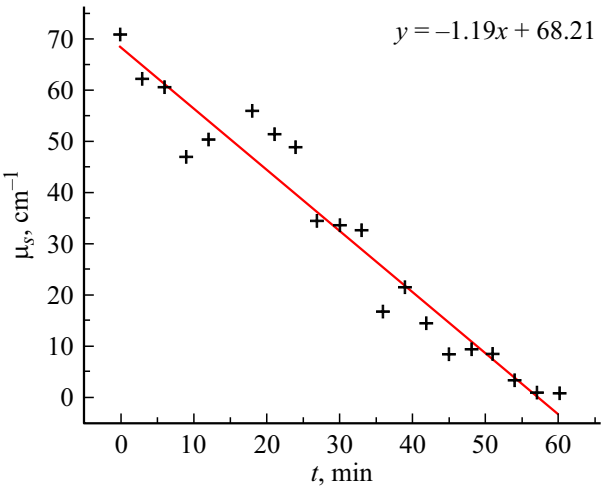

Figure 2. Time dependence of the scattering coefficient μ_s in the dermal area (350−700 μm) of human skin under the action of a clearing agent, obtained from experimental OCT data using the single scattering model approximation of an aqueous solution of glucosamine hydrochloride. The linear approximation is indicated by a solid line and is expressed as an equation.

of the dermal layer of human skin *in vivo* (25 min after applying the optical clearing agent) and the approximating curve, constructed using the single scattering model (equation (3)). OCT signals in the form of A-scans were averaged over the entire scan length of 2 mm along the skin surface. The scattering coefficient values were determined in the area of the averaged A-scan at depths from 350 to 700 μm.

To evaluate the efficiency of optical clearing of the skin *in vivo*, we used the scattering coefficient values obtained using an averaged A-scan in the dermis region at depths from 350 to 700 μm. Figure 2 shows the dependence of the scattering coefficients under the influence of the clearing agent on the observation time. It can be seen that the value of optical clearing over a long time interval is described quite well by the linear regression model (the coefficient of determination R^2 is 88%).

The values of the modulus of the average rate of decrease in the scattering coefficient were used to numerically assess the efficiency of optical clearing (EOC) of human skin. This value is presented as the slope determined from the equation of the regression line (Table 2).

3. Molecular modeling

As in previous works [6,24–27], the structure of the collagen mimetic peptide $\left((GPH)_3\right)_9$ [36] and its shortened version $\left((GPH)_3\right)_2$ were used in the modeling. This peptide represents the largest portion of the regular domains of human collagen. The spatial structure was built according to the Protein Data Bank (PDB). Hydrogen atoms were added

Table 2. Values of intermolecular interaction energies between the collagen fragment $(GPH)_3$ and the studied and compared clearing agents, calculated using the HF/STO-3G/B3LYP/6-311G(d) method, the average number of intermolecular hydrogen bonds N per unit time, and also experimental and predicted values of optical clearing efficiency and their standard deviation errors

№	Optical clearing agent	N, ps^{-1}	ΔE, kJ/mol	EOC, $cm^{-1}min^{-1}$
1	Glucosamine	1.076	−148.9	1.19 ± 0.06 (1.09*, 1.16**)
2	Galactosamine	1.016	−146.0	1.05*, 1.11**
3	1-deoxynodirimycin	1.143	−127.9	0.79*, 1.22**
4	Sucrose	0.812 [26]*	−144.8 [25]	1.05 ± 0.12 [25]
5	Iohexol	0.881	−130.5 [25]	0.78 ± 0.09 [25]

Note. * — optical clearing efficiency values predicted using regression analysis as a function of the energy of intermolecular interaction between clearing agents and a collagen peptide fragment; ** — optical clearing efficiency values predicted by regression analysis as a function of the number of hydrogen bonds between clearing agents and the collagen peptide fragment.

to the model, followed by optimization of the geometric structure using the molecular mechanics method [37]. Molecular models of glucosamine, galactosamine, and 1-deoxynodirimycin were used as clearing agents.

At the initial stage, using the DFT/B3LYP/6-311+G(d,p) [38,39] method, implemented in the Gaussian [40] program, a conformational analysis of the molecular models of the clearing agents under consideration was carried out agents, the minimum energy spatial configurations and the distribution of charges on atoms according to Mulliken were found. To confirm that all molecular models were at local energy minima, vibrational wavenumbers were also calculated and tested for negative values. The relative population of conformers in the mixture was determined by the formula:

$$N_i = \frac{\exp(-F_i/RT)}{\sum_i^n \exp(-F_i/RT)}, \quad (4)$$

where F_i — difference in total electronic energies of conformers, R — universal gas constant, T — absolute temperature (the value of 298.15 K was used in the calculation).

The optimized spatial structure of the most significant conformations of the molecules of glucosamine, galactosamine and 1-deoxynodirimycin are presented in Fig. 3.

Figure 3 shows that low-energy conformers are those with the maximum number of intramolecular hydrogen bonds. Since in this case for each molecule there are several conformers with the same number of intramolecular hydrogen bonds, a complete conformational analysis of all potential configurations was performed to determine the lowest energy conformers. When calculating the energies of intermolecular interaction, only the lowest energy molecular configurations of clearing agents were used.

At the next stage, modeling of the intermolecular interaction of clearing agents with collagen peptides was carried out using the classical molecular dynamics package GROMACS [41] with the AMBER-03 [42] force field. The model scene is a three-dimensional cell in the shape of a rectangular parallelepiped with side lengths: $3 \times 3 \times 9$ nm. The boundaries of the cell were chosen to be periodic (in the case of a collision with the boundary, the molecule passes through it, appearing from the opposite boundary). Before each modeling begins, 20 agent molecules are randomly distributed within the cell. The initial velocities of the atoms were set using a random number generator in the GROMACS package and had a Maxwell distribution corresponding to the selected temperature. To simulate the system, a Berendsen thermostat and barostat [43] were used to ensure the convergence of the temperature and pressure of the system to the set values: $T_0 = 300$ K and $P_0 = 1$ bar. The modeling time step was chosen to be 0.0001 ps, and the total modeling time was 100 ps. The system state was recorded every 0.1 ps. The recorded trajectories of molecular motion were processed using the GROMACS package and the VMD (Visual Molecular Dynamics) program [44]. For each system under study, the modeling was repeated 30 times, and the results were averaged.

When analyzing the trajectories of molecular motion obtained as a result of modeling, it was assumed that a hydrogen bond is formed between atoms if the following geometric criteria are met: $R \leq 3.5$ Å [45] and $\phi \leq 30^\circ$, where R — the distance between the donor atom A, covalently bonded to the hydrogen atom H, and the acceptor B atom of another molecule (or functional group of the same molecule), and ϕ — the angle formed by the AH bonds and AB. An example of such interaction is shown in Fig. 4. As part of this modeling step, the average number of hydrogen bonds formed between low molecular weight agents and collagen per unit time was estimated.

Then, using the HF/STO-3G method, the structural model of the $\left((GPH)_3\right)_2$ collagen peptide fragment, which has a regular structure and consists of 231 atoms, was optimized (Fig. 5) [46].

This optimized model was used for molecular docking with clearing agents using the AutoDockVina [47] program. For each clearing agent, the ten most stable optimized configurations of intermolecular complexes were selected, the structure of which was further optimized by the HF/STO-3G method. The total electron energy was then calculated for each complex using the DFT/B3LYP/6-311G(d) method using a single SCF procedure. The same procedure was used to calculate the total electron energy of the clearing agents and the collagen peptide fragment.

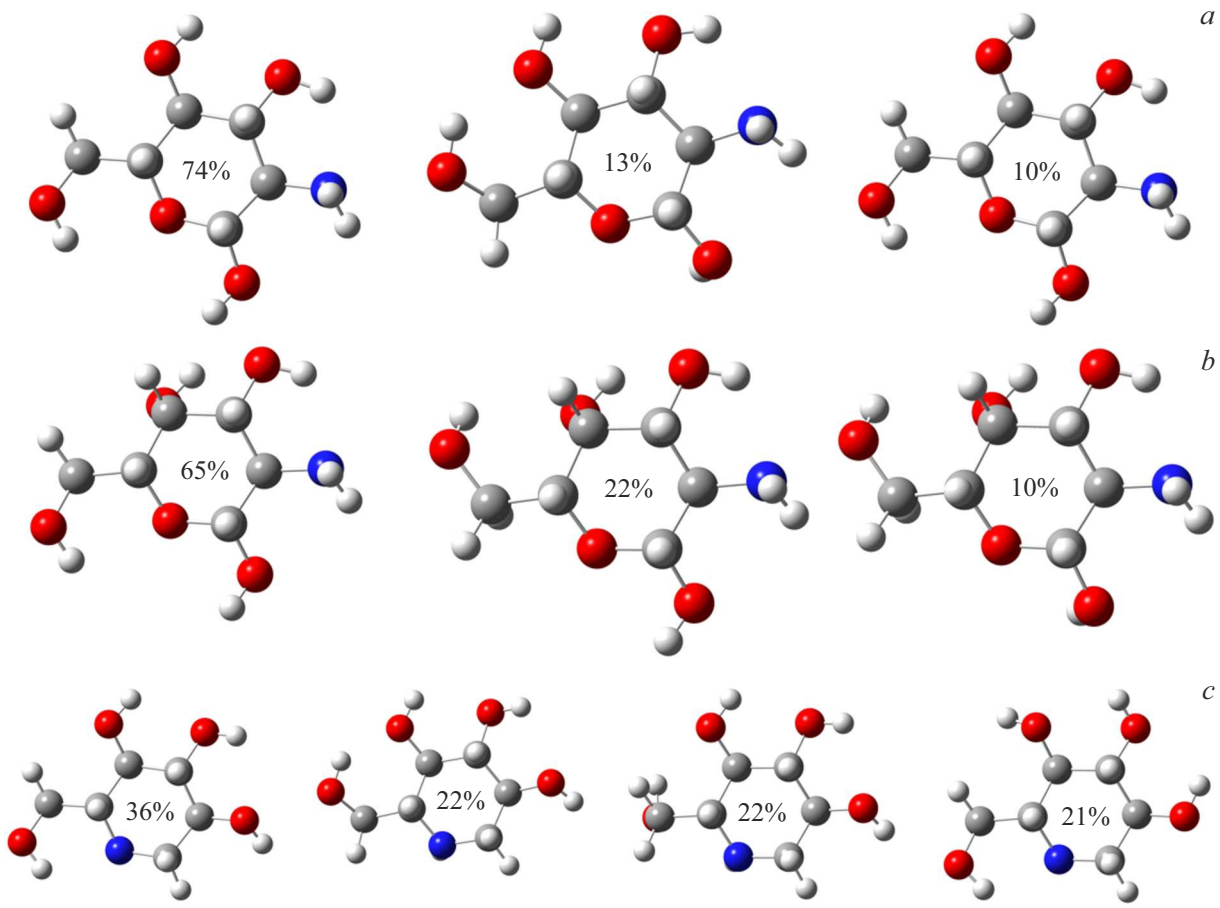

Figure 3. Optimized by the DFT/B3LYP/6-311+G(d,p) method, the spatial structure of the most energy-significant conformations of the molecules glucosamine (*a*), galactosamine (*b*) and 1-deoxynodirimycin (*c*). The numbers in the figure indicate the percentage contribution of each conformer in their total mixture (calculated values were rounded to whole numbers).

The energy of intermolecular interaction was calculated as the difference between the total electronic energy of the complex and the energies of the individual components. The spatial structures of the strongest interaction energy of intermolecular complexes of collagen peptide with molecules of glucosamine, galactosamine, and 1-deoxynodirimycin are shown in Fig. 6.

4. Discussion

As can be seen from Fig. 6, the number of intermolecular hydrogen bonds formed in all clearing agents when interacting with the collagen peptide is the same. The average hydrogen bond length in the glucosamine$-\left((\mathrm{GPH})_3\right)_2$ complex is 1.71 Å, in the similar galatosamine complex — 1.72 Å, in the 1-deoxynodirimycin complex — 1.87 Å. In this case, there is a complete correlation between the strength of intermolecular interaction and the average length of the hydrogen bond. It should be noted that this correlation is not always correct when describing the strength of intermolecular interaction; this also applies to the correlation between the number of hydrogen bonds and the strength of intermolecular interaction [26]. This is due, in particular, to the fact that significant energy can be used for the structural transformation of molecular systems when creating a complex.

The values of intermolecular interaction energies and the efficiency of optical clearing (modulus of the average rate of decrease in the scattering coefficient), obtained using OCT, are given in Table 2.

To plot the dependence of the efficiency of optical clearing of human skin *in vivo* on the energy of intermolecular interaction between clearing agents and a fragment of the collagen peptide $\left((\mathrm{GPH})_3\right)_2$ (Fig. 6) and the average number of hydrogen bonds formed between clearing agents and a fragment of the same peptide (Fig. 7) experimental data from the work [25] were used.

The intermolecular interaction energies presented in Fig. 7 for various complexes of clearing agents with collagen peptide have a noticeable correlation with the efficiency of optical clearing of human skin obtained *in vivo*. The value of the linear correlation coefficient is 0.93. The correlation was constructed using the first six clearing agents. The resulting correlation was used to theoretically predict optical clearing efficiency values for three clearing agents (glucosamine,

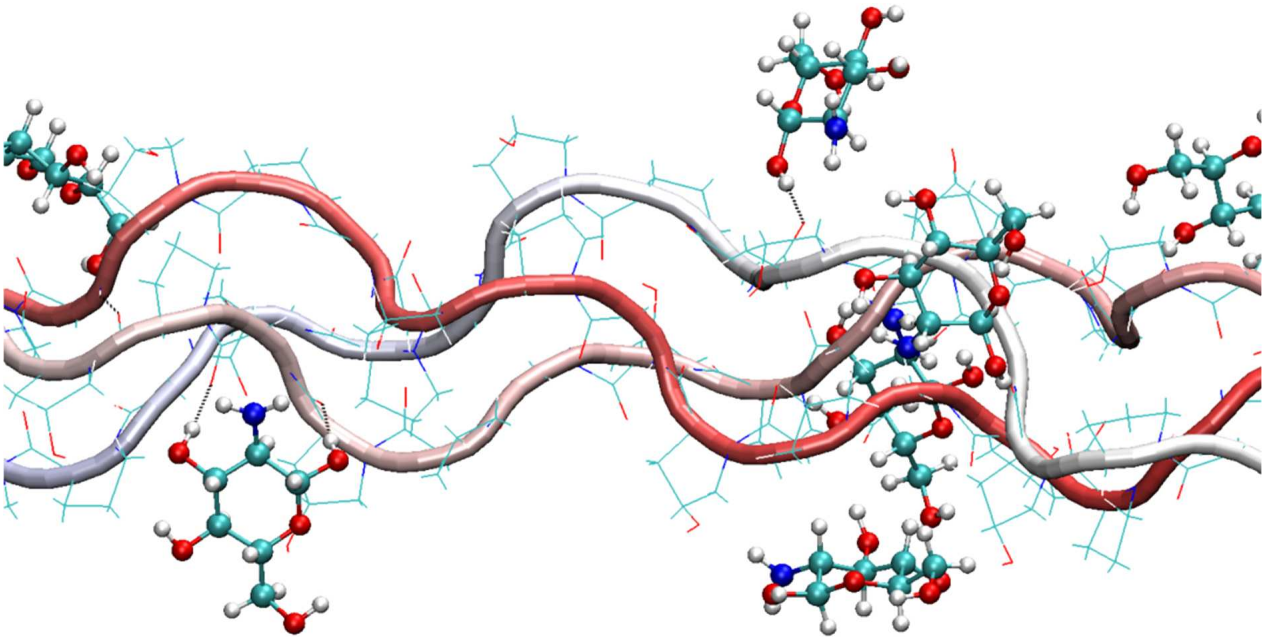

Figure 4. Fragment of the spatial structure of the hydrogen-bonded complex of glucosamine molecules and collagen peptide $\left((\mathrm{GPH})_3\right)_9$, obtained as part of classical molecular dynamics.

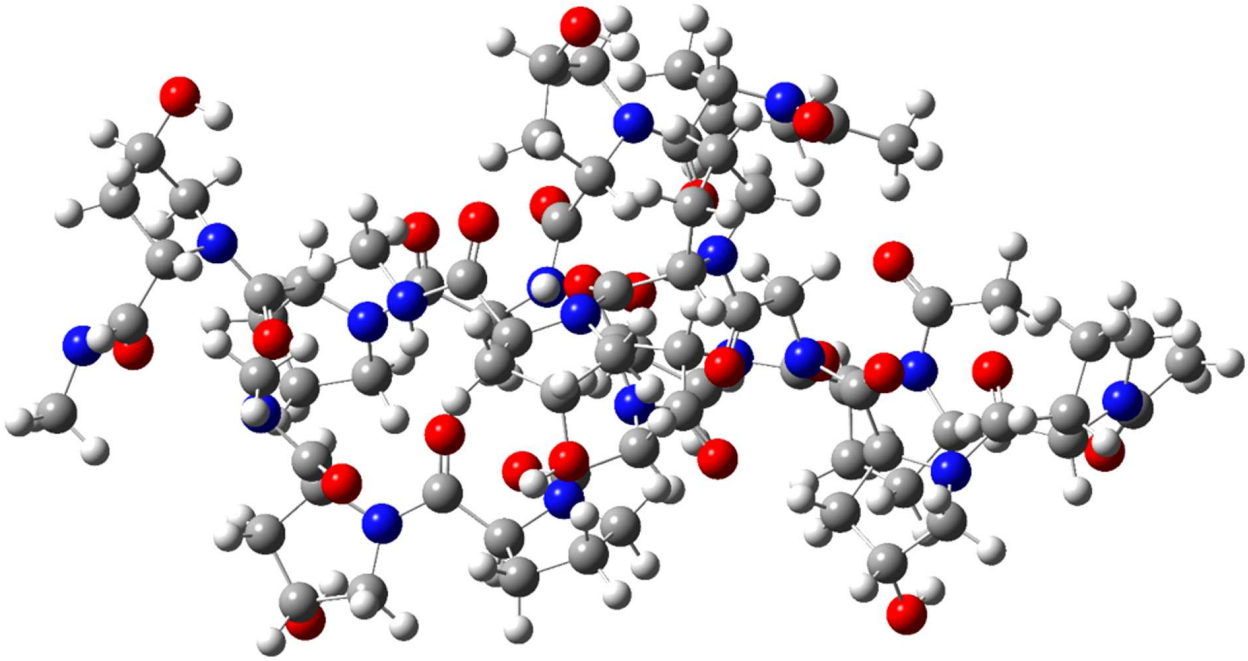

Figure 5. Spatial structure of the $\left((\mathrm{GPH})_3\right)_2$ collagen peptide fragment optimized by the HF/STO-3G method.

galactosamine, 1-deoxynodirimycin). The relative error in theoretically determining the efficiency of optical clearing for glucosamine was 8.2%.

By analogy with the previous dependence, Fig. 8 also presents the results of a regression analysis of the effectiveness of optical clearing of human skin *in vivo* on the number of hydrogen bonds between the clearing agent and the collagen peptide fragment. The value of the linear correlation coefficient is 0.46. By analogy, the resulting correlation was used to theoretically predict optical clearing efficiency values for three clearing agents (glucosamine, galactosamine, 1-deoxynodirimycin). The relative error in theoretically determining the efficiency of optical clearing for glucosamine was 2.5%.

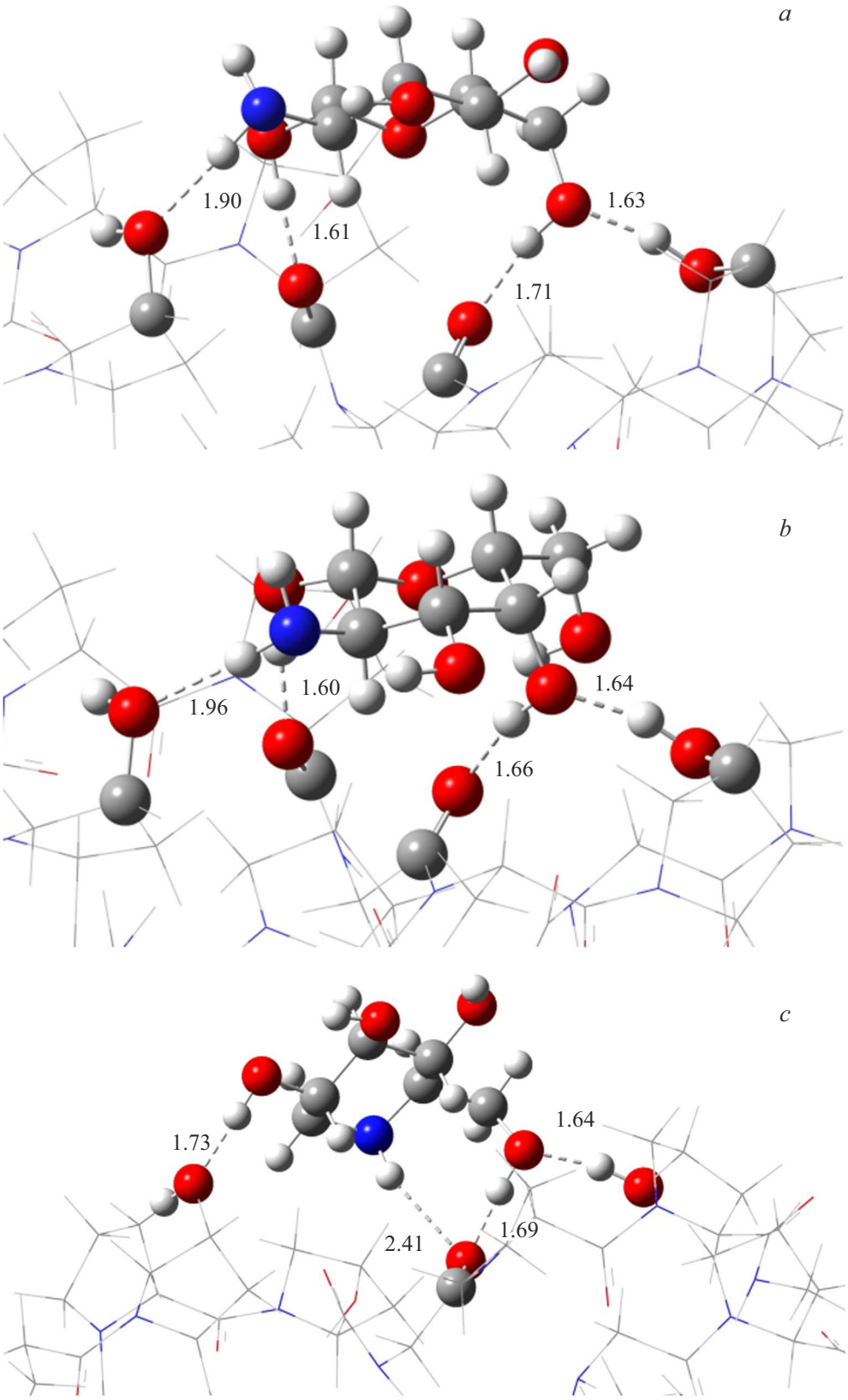

Figure 6. Spatial configurations of fragments of hydrogen-bonded complexes with the maximum value of intermolecular interaction formed by a fragment of the collagen peptide $\left((\mathrm{GPH})_3\right)_2$ and molecules of glucosamine (a), galactosamine (b) and 1-deoxynodirimycin (c) after optimization using the HF/STO-3G method. The dashed line shows intermolecular hydrogen bonds. The numbers in the figure indicate the lengths of hydrogen bonds in angstroms.

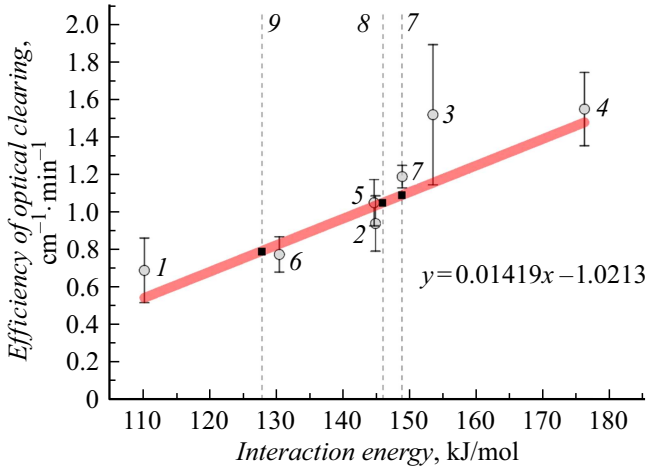

Figure 7. Dependence of the efficiency of optical clearing of human skin *in vivo* on the energy of intermolecular interaction between clearing agents and a fragment of the $\left((\mathrm{GPH})_3\right)_2$ collagen peptide. The numbers *1–6* indicate different types of clearing agents [25]: *1* — glycerin, *2* — ribose, *3* — fructose, *4* — glucose, *5* — sucrose, *6* — iohexol. The numbers *7–9* on the regression line indicate the predicted values of the efficiency of optical clearing for glucosamine, galactosamine and 1-deoxynodirimycin.

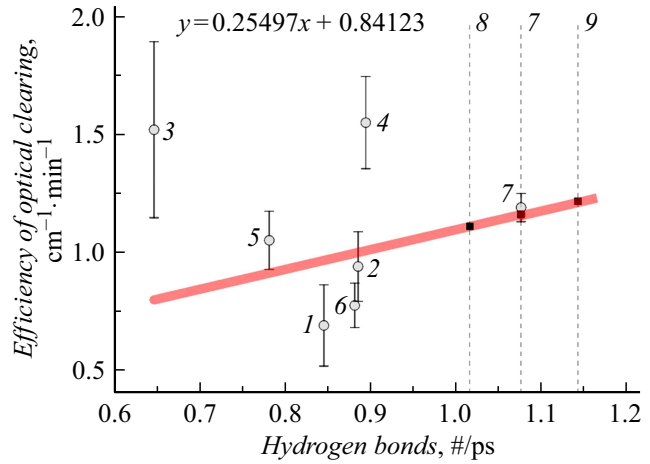

Figure 8. Dependence of the efficiency of optical clearing of human skin *in vivo* on the number of hydrogen bonds between clearing agents and a fragment of the $\left((\mathrm{GPH})_3\right)_2$ collagen peptide. The numbers *1–6* indicate different types of clearing agents [25]: *1* — glycerin, *2* — ribose, *3* — fructose, *4* — glucose, *5* — sucrose, *6* — iohexol. The numbers *7–9* on the regression line indicate the predicted values of the efficiency of optical clearing for glucosamine, galactosamine and 1-deoxynodirimycin.

Despite the fact that the relative error in determining the efficiency of optical clearing of glucosamine using classical molecular dynamics data is smaller, the correlation of parameters in this case is significantly worse than the correlation of parameters obtained using quantum mechanics methods. As already noted in the work [26], this, in our opinion, is due to the fact that classical molecular dynamics, compared to the methods of quantum mechanics, less correctly takes into account the competition between intramolecular and intermolecular hydrogen bonds.

From a comparison of the data given in tables 1 and 2, it is clear that the effectiveness of optical clearing does not directly depend on the value of the refraction index and osmolality. Based on this, we can make a conclusion on the important role of the post-diffusion stage, at which collagen interacts with clearing agents. The results of molecular modeling suggest that the interaction of clearing agents with collagen leads to partial replacement of collagen-bound water. As a result, this leads to reversible dissociation of collagen [21], this, in turn, reduces the average refraction index, which allows to better match their average refraction index with the indices of the intercollagen medium. The higher the affinity of the clear agent for collagen, the more effective the process of optical skin clearing.

Conclusion

In the work, for the first time *in vivo*, the optical clearing efficiency value was established at 60% aqueous solution of glucosamine hydrochloride, which turned out to be close in value to 60% aqueous solution of sucrose. Using methods of classical molecular dynamics and quantum chemistry, the optical clearing efficiency values for galactosamine and 1-deoxynodirimycin molecules were predicted.

Molecular modeling shows that a fundamental step towards increasing the efficiency of intermolecular interactions is the selection of a molecular agent with certain structural characteristics that allow it to interact with two or more molecular pockets of collagen simultaneously, as shown in the work [48] for polyethylene glycol 400. Such an effective clearing agent can be represented by a polymer-type molecular system consisting, for example, of six-atom monosaccharides linked by a mobile carbon-oxygen chain of such a length that allows the saturated sugar rings to reach the molecular pockets of collagen and interact with them through hydroxyl groups. It should be noted that an increase in the size of the molecules used as a clearing agent will lead to an increase in their viscosity and, as a result, to a decrease in the diffusion constant in tissues, as well as an increase in the time required for its leaching from tissues.

Funding

The work has been funded by the grant (№ 23-14-00287) from the Russian Science Foundation.

Conflict of interest

The authors declare that they have no conflict of interest.

References

[1] V.V. Tuchin. *Tissue Optics: Light Scattering Methods and Instruments for Medical Diagnostics,* 3rd ed. (PM 254, SPIE Press, Bellingham, WA, 2015), p. 988.

[2] H. Jonasson, I. Fredriksson, S. Bergstrand, C.J. Östgren, M. Larsson, T. Strömberg. J. Biomed. Opt., **23** (12), 121608 (2018). DOI: 10.1117/1.JBO.23.12.121608

[3] V.V. Tuchin, D. Zhu, E.A. Genina (eds.) *Handbook of Tissue Optical Clearing: New Prospects in Optical Imaging* (Taylor & Francis Group LLC, CRC Press, Boca Raton, FL, 2022), p. 688.

[4] J.M. Hirshburg. *Chemical Agent Induced Reduction of Skin Light Scattering: Doctoral Dissertation* (Texas A&M University, 2009), p. 119.

[5] D. Zhu, K.V. Larin, Q. Luo, V.V. Tuchin. Laser Photon. Rev., **7** (5), 732 (2013). DOI: 10.1002/lpor.201200056

[6] A.N. Bashkatov, K.V. Berezin, K.N. Dvoretskiy, M.L. Chernavina, E.A. Genina, V.D. Genin, V.I. Kochubey, E.N. Lazareva, A.B. Pravdin, M.E. Shvachkina, P.A. Timoshina, D.K. Tuchina, D.D. Yakovlev, D.A. Yakovlev, I.Yu. Yanina, O.S. Zhernovaya, V.V. Tuchin. J. Biomed. Opt., **23** (9), 091416 (2018). DOI: 10.1117/1.JBO.23.9.091416

[7] L. Oliveira, V.V. Tuchin. *The Optical Clearing Method: A New Tool for Clinical Practice and Biomedical Engineering* (Springer Nature Switzerland AG, Basel, 2019), p. 188. DOI: 10.1007/978-3-030-33055-2

[8] I. Costantini, R. Cicchi, L. Silvestri, F. Vanzi, F.S. Pavone. Biomed. Optics Express, **10** (10), 5251 (2019). DOI: 10.1364/boe.10.005251

[9] P. Matryba, L. Kaczmarek, J. Gołąb. Laser Photon. Rev., **13** (8), 1800292 (2019). DOI: 10.1002/lpor.201800292

[10] T. Yu, J. Zhu, D. Li, D. Zhu. Science, **24** (3), 102178 (2021). DOI: 10.1016/j.isci.2021.102178

[11] I.S. Martins, H.F. Silva, E.N. Lazareva, N.V. Chernomyrdin, K.I. Zaytsev, L.M. Oliveira, V.V. Tuchin. Biomed. Optics Express, **14** (1), 249 (2023). DOI: 10.1364/BOE.479320

[12] E.C. Cheshire, R.D.G. Malcomson, S. Joseph, A. Adnan, D. Adlam, G.N. Rutty. Int. J. Legal Med., **131**, 1377 (2017). https://doi.org/10.1007/s00414-017-1570-1

[13] T. Yu, J. Zhu, Y. Li, Y. Ma, J. Wang, X. Cheng, S. Jin, Q. Sun, X. Li, H. Gong, Q. Luo, F. Xu, S. Zhao, D. Zhu. Sci. Rep., **8**, 1964 (2018). DOI: 10.1038/s41598-018-20306-3

[14] X. Wen, S.L. Jacques, V.V. Tuchin, D. Zhu. J. Biomed. Opt., **17** (6), 066022 (2012). DOI: 10.1117/1.JBO.17.6.066022

[15] A.N. Bashkatov, E.A. Genina, V.V. Tuchin. In: *Handbook of Optical Sensing of Glucose in Biological Fluids and Tissues*, ed. by V.V. Tuchin (Taylor & Francis Group LLC, CRC Press, 2009), p. 587.

[16] K.V. Larin, V.V. Tuchin. Quant. Electron., **38** (6), 551 (2008). DOI: 10.1070/QE2008v038n06ABEH013850

[17] D.K. Tuchina, R. Shi, A.N. Bashkatov, E.A. Genina, D. Zhu, Q. Luo, V.V. Tuchin. J. Biophotonics, **8** (4), 332 (2015). DOI: 10.1002/jbio.201400138

[18] V. Hovhannisyan, P.-S. Hu, S.-J. Chen, C.-S. Kim, C.-Y. Dong. J. Biomed. Opt., **18** (4), 046004 (2013). DOI: 10.1117/1.JBO.18.4.046004

[19] A.Yu. Sdobnov, M.E. Darvin, E.A. Genina, A.N. Bashkatov, J. Lademann, V.V. Tuchin. Spectrochimi. Acta Part A: Molecular and Biomolecular Spectroscopy, **197**, 216 (2018). DOI: 10.1016/j.saa.2018.01.085

[20] T. Yu, X. Wen, V.V. Tuchin, Q. Luo, D. Zhu. J. Biomed. Opt., **16** (9), 095002 (2011). DOI: 10.1117/1.3621515

[21] A.T. Yeh, B. Choi, J.S. Nelson, B.J. Tromberg. J. Investigative Dermatology, **121** (6), 1332 (2003). DOI:10.1046/j.1523-1747.2003.12634.x

[22] X. Wen, Z. Mao, Z. Han, V.V. Tuchin, D. Zhu. J. Biophoton., **3** (1−2), 44 (2010). DOI: 10.1002/jbio.200910080

[23] A.Yu. Sdobnov, M.E. Darvin, J. Schleusener, J. Lademann, V.V. Tuchin. J. Biophoton., **12** (5), e201800283 (2019). DOI: 10.1002/jbio.201800283

[24] K.V. Berezin, K.N. Dvoretski, M.L. Chernavina, A.M. Likhter, V.V. Smirnov, I.T. Shagautdinova, E.M. Antonova, E.Yu. Stepanovich, E.A. Dzhalmuhambetova, V.V. Tuchin. J. Mol. Modeling., **24** (2), 45 (2018). DOI: 10.1007/s00894-018-3584-0

[25] K.V. Berezin, E.V. Grabarchuk, A.M. Likhter, K.N. Dvoretskiy, V.V. Tuchin. J. Biophoton., e202300354 (2023). DOI: 10.1002/jbio.202300354

[26] K.V. Berezin, K.N. Dvoretskii, V.V. Nechaev, A.V. Novoselova, A.M. Likhter, I.T. Shagautdinova, E.V. Grabarchuk, V.V. Tuchin. Opt. Spectr., **129** (7), 763 (2021). DOI: 10.1134/S0030400X21060035

[27] K.V. Berezin, K.N. Dvoretskii, M.L. Chernavina, V.V. Nechaev, A.M. Likhter, I.T. Shagautdinova, E.M. Antonova, V.V. Tuchin. Opt. Spectr., **127** (2), 352 (2019). DOI: 10.1134/S0030400X19080071

[28] W.W. Pigman, D. Horton, J.D. Wander. *The Carbohydrates* (Academic Press., NY., 1980), p. 727–728. ISBN: 9780125563512

[29] MedlinePlus, US National Library of Medicine. https://medlineplus.gov/druginfo/natural/807.html

[30] The DailyMed database [Electronic resource]. URL: https://dailymed.nlm.nih.gov/dailymed/fda/fdaDrugXsl.cfm?setid=442aed6e-6242-4a96-90aa-d988b62d55e8&type=display

[31] D.J. Faber, F.J. van der Meer, M.C.G. Aalders, T.G. van Leeuwen. Opt. Express, **12** (19), 4353 (2004). DOI: 10.1364/OPEX.12.004353

[32] P. Lee, W. Gao, X. Zhang. Appl. Opt., **49** (18), 3538 (2010). DOI: 10.1364/AO.49.003538

[33] E.A. Genina, A.N. Bashkatov, E.A. Kolesnikova, M.V. Basko, G.S. Terentyuk, V.V. Tuchin. J. Biomed. Opt., **19** (2), 021109 (2014). DOI: 10.1117/1.JBO.19.2.021109

[34] R.K. Wang, V.V. Tuchin. in: *Handbook of Coherent-Domain Optical Methods. Biomedical Diagnostics, Environmental Monitoring, and Material Science. V. 2, 2nd edition*, ed. by V.V. Tuchin (Heidelberg, Berlin, Springer-Verlag, NY., 2013), v. 2, p. 665.

[35] E.A. Genina, N.S. Ksenofontova, A.N. Bashkatov, G.S. Terentyuk, V.V. Tuchin. Quant. Electron., **47** (6), 561 (2017). DOI: 10.1070/QEL16378

[36] K. Okuyama, K. Miyama, K. Mizuno, H.P. Bachinger. Biopolymers, **97** (8), 607 (2012). DOI: 10.1002/bip.22048

[37] W.D. Cornell, P. Cieplak, C.I. Bayly, I.R. Gould, K.M.Jr. Merz, D.M. Ferguson, D.C. Spellmeyer, T. Fox, J.W. Caldwell, P.A. Kollman. J. Am. Chem. Soc., **117** (19), 5179 (1995). DOI: 10.1021/ja00124a002

[38] A.D. Becke. J. Chem. Phys., **98** (7), 5648 (1993). DOI: 10.1063/1.464913

[39] C. Lee, W. Yang, R.G. Parr. Phys. Rev., **37B** (2), 785 (1988). DOI: 10.1103/PhysRevB.37.785

[40] M.J. Frisch, G.W. Trucks, H.B. Schlegel et al. *Gaussian09, Revision A.02*. (Gaussian, Inc., Pittsburgh PA, 2009)

[41] D. Vander Spoel, E. Lindahl, B. Hess, G. Groenhof, E.A. Mark, H.J.C. Berendsen, J. Comput. Chem., **26** (16), 1701 (2005). DOI: 10.1002/jcc.20291

[42] Y. Duan, C. Wu, S. Chowdhury, M.C. Lee, G. Xiong, W. Zhang, R. Yang, P. Cieplak, R. Luo, T. Lee, J. Caldwell, J. Wang, P. Kollman. J. Comp. Chem., **24** (16), 1999 (2003). DOI: 10.1002/jcc.10349
[43] H.J.C. Berendsen, J.P.M. Postma, W.F. van Gunsteren, A. DiNola, J.R. Haak. J. Chem. Phys., **81** (8), 3884 (1984). DOI: 10.1063/1.448118
[44] W. Humphrey, A. Dalke, K. Schulten. J. Mol. Graph., **14** (1), 33 (1996). DOI: 10.1016/0263-7855(96)00018-5
[45] H.D. Loof, L. Nilsson, R. Rigler. J. Am. Chem. Soc., **114** (11), 4028 (1992). DOI: 0.1021/ja00037a002
[46] C.C.J. Roothaan. Rev. Mod. Phys., **23** (2), 69 (1951). DOI: 10.1103/REVMODPHYS.23.69
[47] Y. Duan, C. Wu, S. Chowdhury, M.C. Lee, G. Xiong, W. Zhang, R. Yang, P. Cieplak, R. Luo, T. Lee, J. Caldwell, J. Wang, P. Kollman. J. Comp. Chem., **24** (16), 1999 (2003). DOI: 10.1002/jcc.10349
[48] K.V. Berezin, K.N. Dvoretskiy, V.V. Nechaev, A.M. Likhter, I.T. Shagautdinova, V.V. Tuchin. J. Biomed. Photon. Eng., **6** (2), 20308 (2020). DOI: 10.18287/JBPE20.06.020308

Translated by A.Akhtyamov